Electronic Supplementary Information

# Unexpected effects of Zr-doping in the high performance sodium manganese-based layer-tunnel cathode

**Jie Qu, [a] Tian sheng, [b] Zhen-guo Wu, [*a,c] Ting-ru Chen, [a] Hui Chen, [a] Zu-guang Yang, [a] Xiao-dong Guo, [*a,e] Jun-tao Li, [d] Benhe Zhong, [a] Xue-shi Dou, [e]**

[a] *College of Chemical Engineering, Sichuan University, Chengdu 610065, P. R. China;.*

[b] *College of Chemistry and Materials Science, Anhui Normal University, Wuhu, 241000, P. R. China;*

[c] *State Key Laboratory of Physical Chemistry of Solid Surfaces, College of Chemistry and Chemical Engineering, Xiamen University, Xiamen, 361005 (PR China);*

[d] *College of Energy, Xiamen University, Xiamen, 361005 (PR China);*

[e] *Institute for Superconducting and Electronic Materials, University of Wollongong, Wollongong, NSW 2522 (Australia);*

**TableS1** Results of structural analysis obtained from X-ray Rietveld refinement of the prepared samples

| | **Zr-0** | | **Zr-0.02** | | **Zr-0.05** | |
|---|---|---|---|---|---|---|
| space group | *pbam* | *P63/mmc* | *pbam* | *P63/mmc* | *pbam* | *P63/mmc* |
| lattice parameters (Å) | a= 9.1682 | a=2.8689 | a=9.1737 | a=2.8832 | a=9.1706 | a=2.8713 |
| | b=26.6852 | b=2.8689 | b=26.7832 | b=2.8832 | c=26.6983 | b=2.8713 |
| | c=2.8265 | c=11.2386 | c=2.8348 | c=11.2596 | c=2.8234 | c=11.2403 |
| mass ratio (%) | 34.6 | 66.4 | 30.4 | 69.6 | 28.2 | 71.8 |
| $R_{wp}$ (%) | 6.61 | | 5.96 | | 6.94 | |
| $R_p$ (%) | 4.95 | | 7.25 | | 7.24 | |

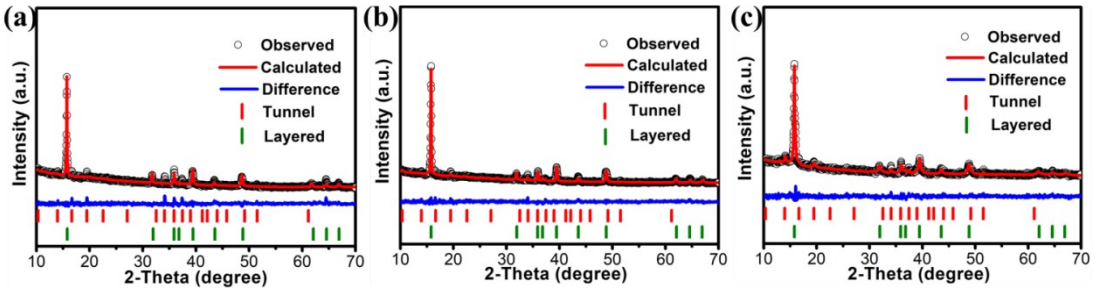


**Figure S1** Rietveld refinement of the as-synthesized (a)Zr-0, (b) Zr-0.02, (c) Zr-0.05.

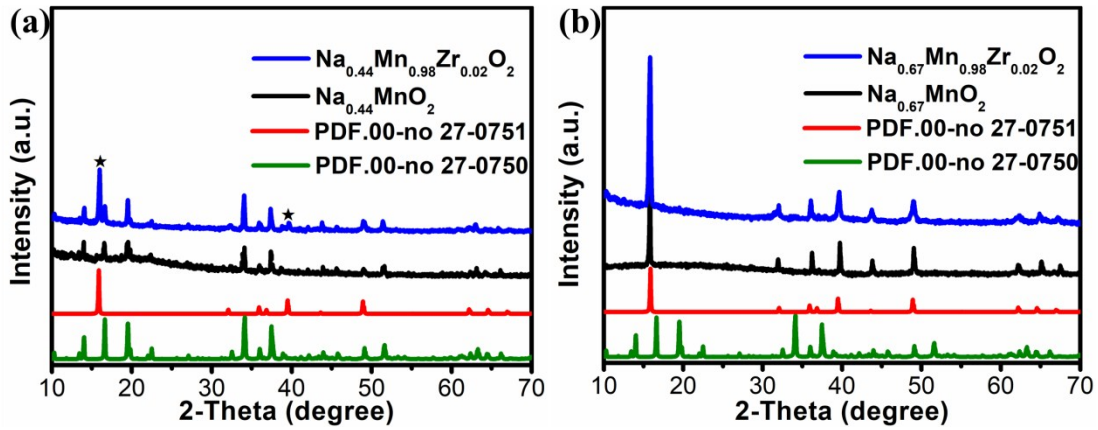


**Figure S2.** The XRD patterns of $Na_{0.44}MnO_2$ (a) and $Na_{0.44}Mn_{0.98}Zr_{0.02}O_2$(b)

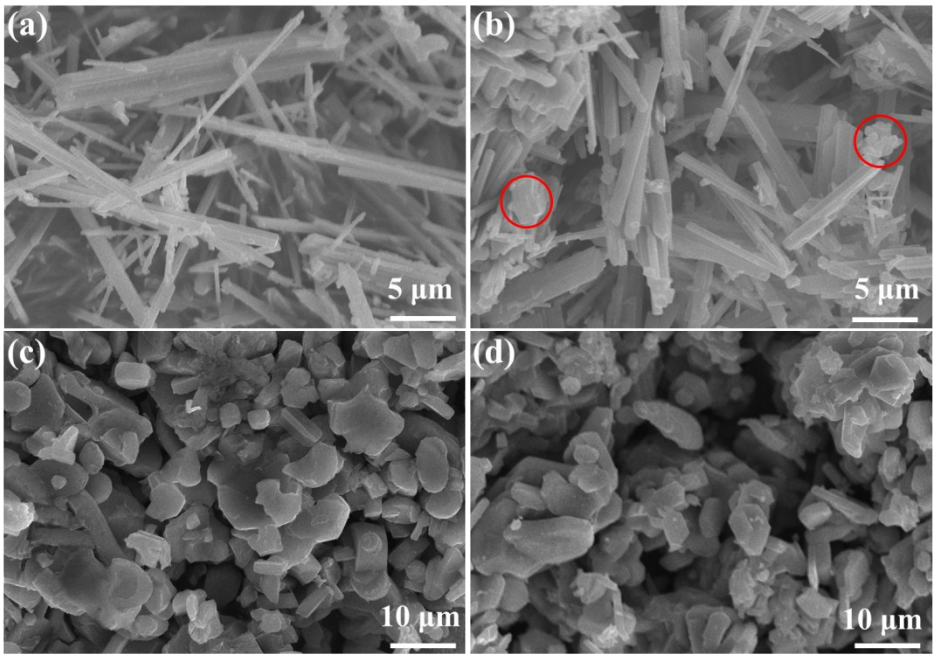


**Figure S3**. The sem images of $Na_{0.44}MnO_2$ (a), $Na_{0.44}Mn_{0.98}Zr_{0.02}O_2$ (b), $Na_{0.67}MnO_2$ (c), and $Na_{0.67}Mn_{0.98}Zr_{0.02}O_2$ (d).

**Computational methods**

The spin-polarized electronic structure calculations were carried out using the Vienna Ab-initio Simulation Package (VASP) code with Perdew-Burke-Ernzerhof (PBE) functional of exchange-correlation.[1-5] The projector-augmented-wave (PAW) pseudopotentials were utilized to describe the core electron interaction. The on-site Coulomb repulsion correction term ($U_{eff}$ = 4.0 eV) determined by linear response theory was used in the 3d electrons of Mn.[6,7] The layered $Na_{0.6}MnO_2$ model consists of 22 Na, 36 Mn and 72 O atoms, as shown in Figure a, corresponding to 36 $MnO_2$ formula unit (f. u.). For the layered structure, the one and two Zr atom doped structures equal to the stoichiometric $Na_{0.611}Mn_{0.972}Zr_{0.028}O_2$ and $Na_{0.611}Mn_{0.944}Zr_{0.056}O_2$, respectively. The tunnel $Na_{0.6}MnO_2$ model consists of 32 Na, 54 Mn and 108 O atoms, corresponding to 54 $MnO_2$ formula unit (f. u.). For the tunnel structure, the one and two Zr atom doped structures equal to the stoichiometric $Na_{0.593}Mn_{0.981}Zr_{0.019}O_2$ and $Na_{0.593}Mn_{0.963}Zr_{0.037}O_2$, respectively. The cut-off energy was 500 eV and the Monkhorst-Pack k-point sampling was 2×2×1 for both layered and tunnel $Na_{0.66}MnO_2$. For the Zr doped tunnel $Na_{0.6}MnO_2$, the most stable position for Zr atom are examined at all five different Mn positions, and the most

stable position were presented as presented in **Figure S4b**.

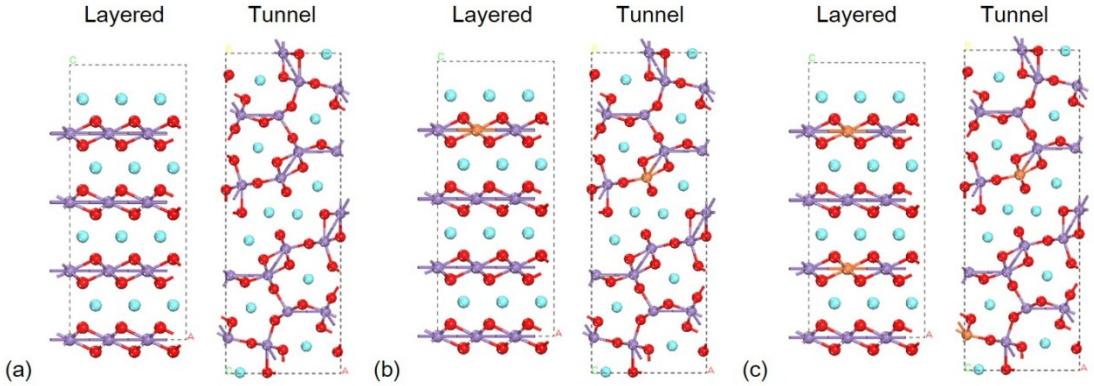


**Figure S4**. Theoretical models of (a) pristine, (b) one Zr atom doped, (c) two Zr atoms doped, layered and tunnel $NaMnO_2$ structures. Purple: Mn; red: O; light green: Na; orange: Zr.

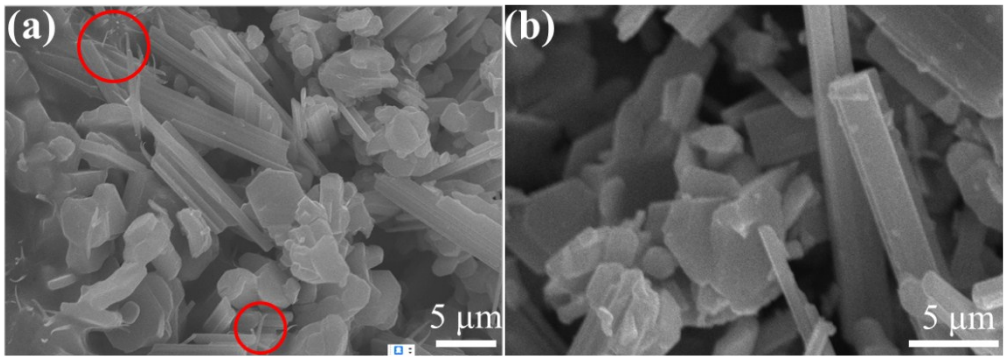


**Figure S5**. The sem images of Zr-0 (a) and Zr-0-rinsed (b)

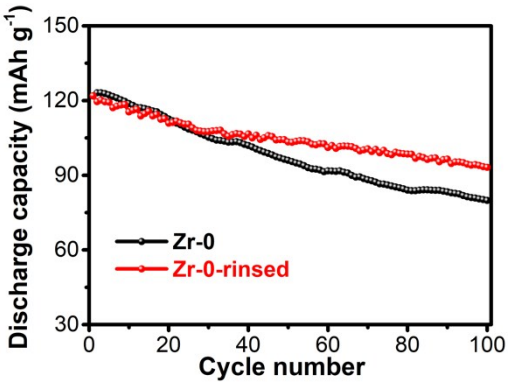


**Figure S6**. The cycling performances of Zr-0 and Zr-0-rinsed at 1 C.

**Table S2** ICP-AES results of $Na_{0.6}Mn_{1-x}Zr_xO_2$ (x=0,0.02,0.05)

| samples | Measured atomic ratio | | |
|---|---|---|---|
| | Na | Mn | Zr |
| x=0 | 0.598 | 0.996 | 0 |
| x=0.02 | 0.602 | 0.975 | 0.018 |
| x=0.05 | 0.605 | 0.951 | 0.052 |

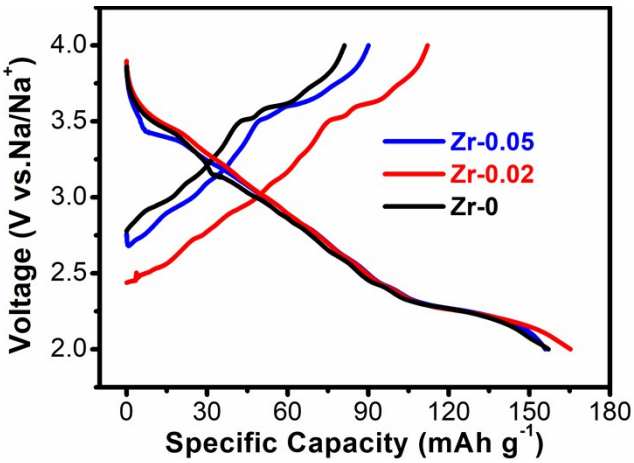


**Figure S7**. The first charge-discharge curves of Zr-0, Zr-0.02 and Zr-0.02 at 0.2 C

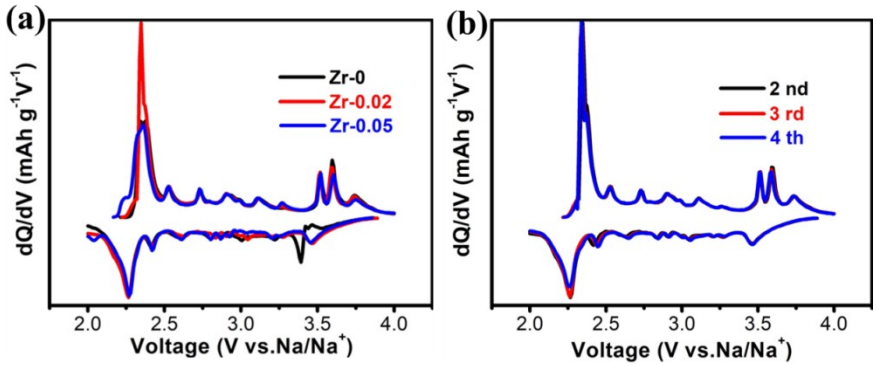


**Figure S8**.(a) The second dq/dv plots of Zr-0, Zr-0.02, Zr-0.05 between 2.0 and 4.0 V at 0.2 C. (b) dq/dv plots of at 0.2 C of Zr-0.02 in the initial cycles.

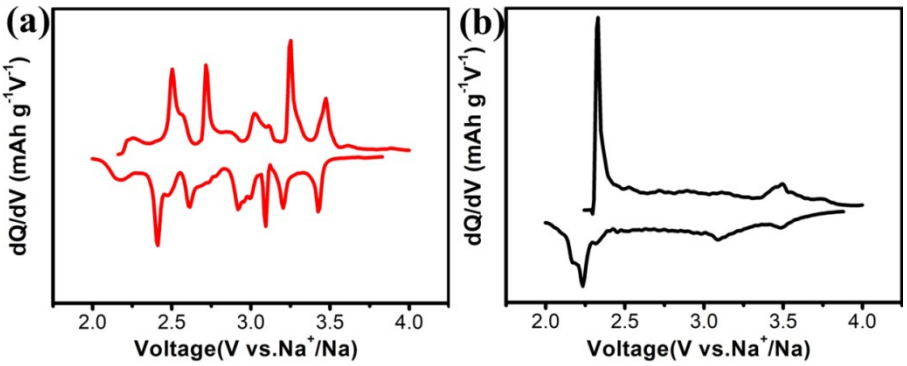


**Figure S9**. The dq/dv curves of $Na_{0.44}MnO_2$ (a) and $Na_{0.67}MnO_2$ (b) at 0.2 C in the second cycle.

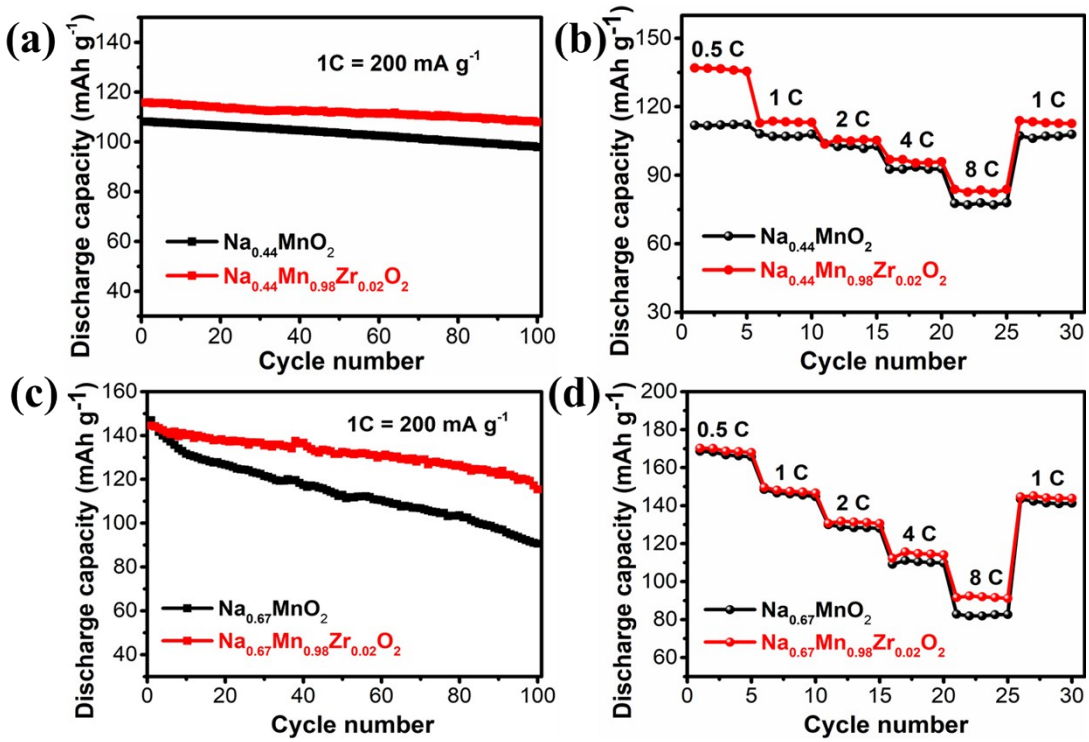


**Figure S10**. The electrochemical performances comparisons between $Na_{0.44}MnO_2$ and $Na_{0.44}Mn_{0.98}Zr_{0.02}O_2$ (a-b), $Na_{0.67}MnO_2$ and $Na_{0.67}Mn_{0.98}Zr_{0.02}O_2$ (c-d).）

**Table S3.** The comparisons on $Na^+$ storage performances between some literatures about layered metal oxides-based cathodes and Zr-0.02

| cathode materials | **rate capability** | **cycling stability** | Reference |
|---|---|---|---|
| P2-$Na_{0.7}CoO_2$ | 64 mAh $g^{-1}$ at 2000 mA $g^{-1}$ | 86% after 300 cycles at 50 mA $g^{-1}$ | 4 |
| P2/O3-$Na_{0.66}Li_{0.18}Mn_{0.71}Co_{0.08}O_2$ | 69 mAh $g^{-1}$ at 500 mA $g^{-1}$ | 75% after 150 cycles at 50 mA $g^{-1}$ | 5 |
| P2-$Na_{0.66}Ni_{0.26}Mn_{0.67}Zn_{0.07}O_2$ | 79 mAh $g^{-1}$ at 768 mA $g^{-1}$ | 83% after 30 cycles at 12 mA $g^{-1}$ | 6 |
| P2/O3-$Na_{0.67}Li_{0.18}Mn_{0.8}Cu_{0.2}O_2$ | 30 mAh $g^{-1}$ at 1205 mA $g^{-1}$ | 65.5% after 100 cycles at 241 mA $g^{-1}$ | 7 |
| P2-$Na_{0.67}Cu_{0.14}Mn_{0.86}O_2$ | 89.6 mAh $g^{-1}$ at 1000 mA $g^{-1}$ | 63.3% after 500 cycles at 1000 mA $g^{-1}$ | 8 |
| P2-$Na_{0.67}Mn_{0.8}Fe_{0.1}Ti_{0.1}O_2$ | 45 mAh $g^{-1}$ at 2450 mA $g^{-1}$ | 70% after 300 cycles at 245 mA $g^{-1}$ | 9 |
| P2/T-$Na_{0.6}Mn_{0.98}Zr_{0.02}O_2$ | **81** mAh $g^{-1}$ at **2000** mA $g^{-1}$ | **75%** after **1000** cycles at **2000** mA $g^{-1}$ | this work |

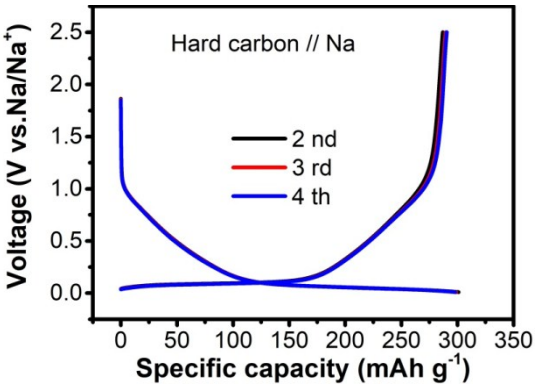


**Figure S11**. The initial charge-discharge profiles of hard carbon anode between 0.01 and 2.5 V (vs $Na/Na^+$)

**Table S4**. The fitting results of equivalent circuit from EIS curves at room temperatures

| Samples | $R_{ct}$/Ω | $D_{Na^+}$/($cm^2$ $s^{-1}$) | chi^2 (%) | Errors (%) |
|---|---|---|---|---|
| Zr-0 | 178.3 | 5.42×10-14 | 0.2865 | 1.6874 |
| Zr-0.02 | 89.4 | 8.62×10-14 | 0.2962 | 2.3555 |
| Zr-0.05 | 146.65 | 4.18×10-14, | 0.1985 | 1.4856 |

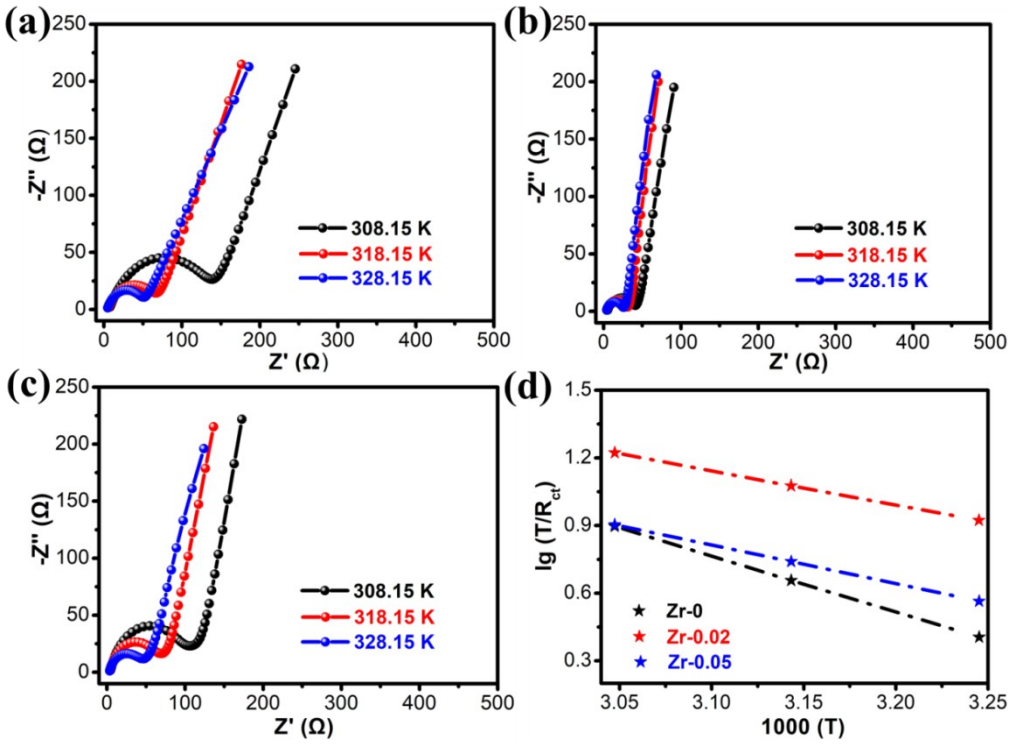


**Figure S12**. The Nyquist plots of Zr-0 (a), Zr-0.02 (b), Zr-0.05 (c) at different temperature after cycling at a current density of 200 mA $g^{-1}$ for 100 circles. The plots of ln ($T/R_{ct}$) as a function of 1000/$T$ for Zr-0, Zr-0.02 and Zr-0.05 (d).

**Equation S1**: $\frac{T}{R_{ct}} = Aexp(-\frac{E_a}{RT})$

where $E_a$ is the activation energy, $T$ the absolute temperature, $R$ the gas constant, $R_{ct}$ is the interfacial sodium-ion transfer resistance, and $A$ the pre-exponential factor.

**Table S5** Fitting results of equivalent circuit from Nyquist curves for the samples

| Sample | Temperature ($K$) | $R_s$ (Ω) | $R_{ct}$ (Ω) |
|---|---|---|---|
| Zr-0 | 308.15 | 6.673 | 149.8 |
| | 318.15 | 4.73 | 76.26 |
| | 328.15 | 4.178 | 56.36 |
| Zr-0.02 | 308.15 | 4.447 | 39.18 |
| | 318.15 | 3.806 | 28.2 |
| | 328.15 | 3.522 | 23.02 |
| Zr-0.05 | 308.15 | 4.178 | 108.3 |
| | 318.15 | 3.617 | 70.66 |
| | 328.15 | 3.015 | 47.34 |

**Equation S2**: $E_a = -Rkln10$

It is clear that $E_a$ is in proportion to $k$. The values of $E_a$ were calculated to be 47.57, 28.98, 32.82 kJ mol$^{-1}$ in Zr-0, Zr-0.02, Zr-0.05.

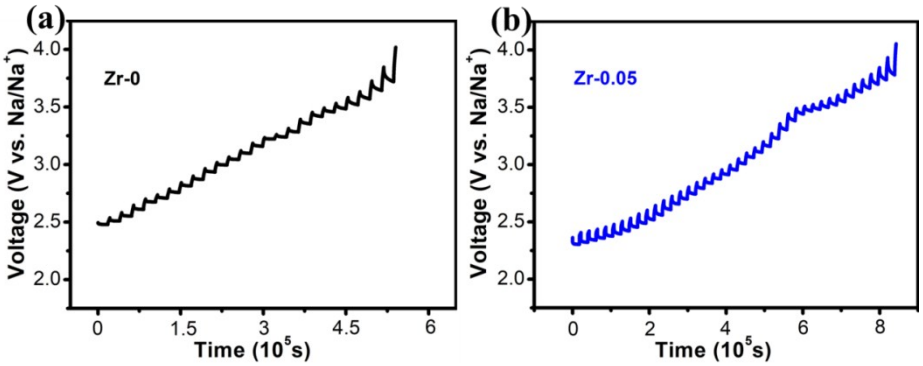


**Figure S13**. GITT curves of Zr-0 (a) and Zr- 0.05 (b) for the first charge process between 2.0 V and 4.0 V

**Table S6** The calculated average $\bar{D}$ values from the GITT tests for the Zr-0, Zr-0.02 and Zr-0.05

| Sample | $\bar{D}/cm^2\ s^{-1}$ |
|---|---|
| Zr-0 | $1.53\times10^{-14}$ |
| Zr-0.02 | $2.72\times10^{-14}$ |
| Zr-0.05 | $1.66\times10^{-14}$, |

References


1. G. Kresse, J. Hafner, Physical. Review. B 1993, **48**, 13115-13118.
2. G. Kresse, J. Furthmuler, Physical. Review. B 1996, **54**, 11169-11186.
3. P. E. Blochl, Physical. Review. B 1994, **50**, 17953-17979.
4. G. Kresse, D. Joubert, Physical. Review. B 1999, **59**, 1758-1775.
5. J. P. Pedrew, K. Burke, M. Ernzerhof, Physical. Review. Letters. 1996, **77**, 3865-3868.
6. M. Cococcioni, S. de Gironcoli, Physical. Review. B 2005, **71**, 035105.
7. C. Franchini, R. Podloucky, J. Paier, M. Marsman, G. Kresse, Physical. Review. B 2007, **75**, 195128.
8. Y. J Fang, X. Y Yu, X. W. Lou, *Angewandte Chemie International Edition*, 2017, **56**, 5801.
9. S. Guo, P. Liu, H. Yu, Y. Zhu, M. Chen, M. Ishida and H. Zhou, *Angewandte Chemie*, 2015, **54**, 5894-5899.
10. X. Wu, J. Guo, D. Wang, G. Zhong, M. J. McDonald and Y. Yang, *Journal of Power Sources*, 2015, **281**, 18-26.
11. M. Bianchini, E. Gonzalo, N. E. Drewett, N. Ortiz-Vitoriano, J. M. López del Amo, F. J. Bonilla, B. Acebedo and T. Rojo, *Journal of Materials Chemistry A*, 2018, **6**, 3552-3559.
12. W. Kang, Z. Zhang, P.-K. Lee, T.-W. Ng, W. Li, Y. Tang, W. Zhang, C.-S. Lee and D. Y. Wai Yu, Journal of Materials Chemistry A, 2015, 3, 22846-22852.
13. M. H. Han, E. Gonzalo, N. Sharma, J. M. López del Amo, M. Armand, M. Avdeev, J. J. Saiz Garitaonandia and T. Rojo, *Chemistry of Materials*, 2015, **28**, 106-116.